BERK TIRNAKCI
YAVUZ SALT

Department of Chemical Engineering, Faculty of Chemical and Metallurgical, Yildiz Technical University, Davutpasa Campus, Esenler-Istanbul, Turkey

PREPARATION AND CHARACTERIZATION OF PVA-SIO$_2$ NANOCOMPOSITE MEMBRANES FOR SEAWATER DESALINATION BY PERVAPORATION

Article Highlights
- For PVA-SiO$_2$ membrane, a permeate flux of 4.93 kg m^{-2} h^{-1} was obtained at 50 °C
- The highest selectivity value was calculated as 99.8% at 30 °C
- The nano-SiO$_2$ incorporation into a PVA matrix increased the water flux value more than two-fold
- The pervaporation performance of PVA membrane was enhanced remarkably

Abstract

Pervaporation is a membrane process that offers high separation performance and has an important potential for the treatment of saline water sources. In this study, poly(vinyl alcohol) (PVA) and PVA-SiO$_2$ nanocomposite membranes were prepared by the solution-casting method, and pervaporative water desalination studies were carried out for synthetic seawater (35 g L^{-1}) at 30, 40 and 50 °C. Effects of the temperatures and the incorporation of SiO$_2$ on the pervaporation performance of polymeric nanocomposite membranes were investigated. Membranes were characterized by scanning electron microscopy (SEM), Fourier-transform infrared spectroscopy (FT-IR) and thermogravimetric analysis (TGA). In experiments conducted at 50 °C, a permeate flux of 4.93 kg m^{-2} h^{-1} with a salt rejection of 99.3% were obtained. The highest salt rejection was 99.8% at temperature of 30 °C. The results showed that the pervaporation performance of PVA membranes was remarkably enhanced with the incorporation of nano-SiO$_2$ into polymeric matrix.

Keywords: desalination, nano-SiO$_2$, nanocomposite, pervaporation, poly(vinyl alcohol), seawater.

Freshwater demand is rapidly increasing for industrial, agricultural, and domestic use. In addition, the amount of water per capita is decreasing rapidly due to the lack of underground and surface water resources (about 1% of all water sources), increased industrialization, global warming, and population growth rate. Seawater is the most abundant water source compared to other natural freshwater resources, and seawater desalination is an important process for meeting freshwater demands. Among

desalination technologies, membrane-based technologies are becoming increasingly important as membrane processes have advantages such as great separation performance, energy-saving, high operational stability, and easy integration with industrial systems [1,2].

For the desalination of seawater and brackish water, reverse osmosis (RO), multi-stage flash (MSF), multi-effect distillation (MED), electrodialysis (ED) and vapor compression distillation (VCD) technologies are commonly used worldwide [3,4]. RO and MSF dominate the market, together constituting >90% of the global desalination capacity [5]. However, RO has major disadvantages such as high capital and operating costs, high energy requirements, and membrane fouling [6].

PV is a promising membrane process for desalination studies due to its non-pressure-driven separ-

ation mechanism, high selectivity, energy efficiency, and durability for pollutants [7]. In this process, the driving force is the chemical potential gradient between the two sides of the membrane, applying either vacuum or sweeping gas at the permeate side of the membrane [8]. The transport mechanism through the nonporous membrane is explained by the solution-diffusion model consisting of three steps: sorption, diffusion and desorption. The feed liquid is brought into contact with one side of the membrane at atmospheric pressure and permeate is continuously removed in vapour form from its other side [9].

The key component in pervaporation as with all other membrane processes is the membrane itself and selecting an appropriate membrane material is a crucial step in membrane studies. In the pervaporation process, water-selective membranes are prepared using polymers with hydrophilic characteristics. For the pervaporation separation of water from feed mixture, PVA is one of the best choices due to its high hydrophilic nature, which is provided by the hydroxyl (-OH) groups on its chain segments. Additionally, PVA has excellent membrane-forming properties, good thermal stability, chemical and mechanical strength, and commercial availability and is nontoxic, biocompatible and biodegradable [8,10].

Inorganic fillers can be incorporated into polymeric matrices to improve the membrane separation performance. Inorganic-organic composite membranes prepared using materials with different structures and properties, namely mixed matrix membranes (MMMs), combine the separation properties of inorganic and organic materials [11,12]. Nanocomposites have an important role in membrane applications. In membrane technology, inorganic nanomaterials such as TiO_2, SiO_2, Al_2O_3, Si, Ag, ZnO and ZrO_2 and organic nano-materials such as graphene oxide (GO), carbon nanotubes (CNT), and carbon nanofibers (CNF) are used as nano-sized fillers to provide thermal, physical, and chemical resistance and improve the membrane separation performance [13,14].

Xie *et al.* [15] prepared PVA/maleic anhydride/ /silica hybrid membranes via the sol-gel method and investigated the effects of temperature, salinity and pressure on the desalination of a NaCl/water solution. They reported a water flux of 11.7 kg m^{-2} h^{-1} and salt rejection values of 99.9% with hybrid membranes containing silica particles (<10 nm) for the pervaporation desalination of NaCl/water solution with NaCl concentrations of 0.2-5.0 wt.% at permeate pressures of 2-40 Torr and temperatures of 20-65 °C. In another study, they also investigated the effect of the thickness of PVA/maleic anhydride/silica membrane on

the desalination performance [16] and obtained a water flux of 6.93 kg m^{-2} h^{-1} with >99.5% salt rejection at 22 °C and 6 Torr for a 2000 ppm NaCl solution. Cho *et al.* [17] prepared an inorganic NaA zeolite membrane for the pervaporative desalination of seawater. Water flux and salt rejection were 1.9 kg m^{-2} h^{-1} and 99.9%, respectively. Chaudhri *et al.* [18] prepared hollow-fiber PVA membranes on a polysulfone support and reported a water flux of approximately 7.4 L m^{-2} h^{-1} at 71 °C. Liang *et al.* [19] used the electrospinning/electrospraying technique to prepare thin-film nanofibrous pervaporation composite (TFNPVC) membranes using poly(vinyl alcohol), polyacrylonitrile (PAN) nanofibrous scaffold and polyethylene terephthalate (PET) to make a three-layered composite membrane. They obtained water fluxes of 8.53, 7.24 and 5.57 L m^{-2} h^{-1} for 5000, 35000 and 50000 ppm NaCl solutions, respectively, with salt rejection of > 99.5%.

In the present study, a nano SiO_2-filled PVA membrane was prepared by the solution-casting method and pervaporation desalination studies were carried out at different temperatures. Glutaraldehyde (GA) was used as the cross-linking agent for PVA. The effects of temperature and nano-SiO_2 incorporation on pervaporation performance were investigated for synthetic seawater desalination. Experiments were carried out at 30, 40, and 50 °C and the permeate flux, rejection, permeance and selectivity results were compared with pristine PVA membranes [20].

EXPERIMENTAL

Materials

PVA (98-99% hydrolyzed, average M.W. 88000- -97000) and GA (25% aq. sln.) were purchased from Alfa Aesar. GA was used as the cross-linking agent for PVA. Sulfuric acid was used as a catalyst for cross-linking reaction, and sulfuric acid and methanol were purchased from J.T. Baker and Lab Scan, respectively. Sodium chloride (NaCl) was purchased from Merck. SiO_2 (99.65%, P-Type) with a particle size of 13-23 nm was supplied by Nanografi Nano Technology. Synthetic seawater (35 g L^{-1}) was prepared in the laboratory.

Membrane preparation

In this study, pristine PVA and PVA-SiO_2 nanocomposite membranes were prepared by a solution casting method. PVA (10 wt.%) was dissolved in deionized water by mixing at a moderate stirring speed for 2 h in a glass reactor placed in a water bath at 90 °C. Subsequently, nano-SiO_2 solution was added to the PVA solution while stirring, and the

whole solution was stirred again for a further 1 hour to ensure a well dispersion. SiO$_2$ nanoparticle was incorporated into polymer matrix in an amount of 10 wt.% with respect to weight of PVA to avoid an agglomeration of the nanoparticles, and a brittle membrane. The nanomaterial was dispersed in water using a magnetic stirrer and an ultrasonic bath before adding it to the polymer solution. The membrane solution was cast onto glass plates as a thin film and was then dried at 40 °C for 24 h. The drying temperature was determined as 40 °C, as the changes in ambient temperature can affect the membrane drying process. The dried membranes were peeled-off from the glass plates and were immersed in a mixture containing 3% GA, 5% H$_2$SO$_4$, 23% water, 69% methanol for 24 h and were cross-linked [21]. The cross-linked membranes were removed from the mixture. Figure 1 shows a schematic representation of the cross-linking reaction between PVA and GA [22].
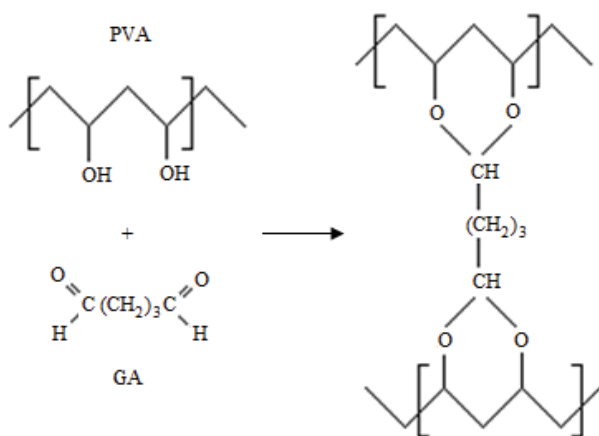

Figure 1. Cross-linking reaction between PVA and GA [22].

The membranes were weighed, and then kept in deionized (DI) water overnight to remove the residues of the cross-linking mixture. After washing with deionized water, the membranes were dried again in an oven at 105 °C for 2 h to remove the water content of the membranes [23]. There was no weight loss in the prepared membranes. For the pristine PVA membranes, the PVA solution (10 wt.%) was prepared by stirring at a moderate speed for 3 h in a reactor placed in a water bath at 90 °C. The membrane solution was cast onto glass plates, and the resulting membrane films were dried at 40 °C for 24 h. A similar procedure was used to prepare the pristine PVA membranes. The membrane thicknesses were measured with a digital micrometer, and the flux values were normalized to 100 μm.

Characterization

Scanning electron microscopy (SEM)

Cross-sectional morphologies of the PVA and PVA-SiO$_2$ nanocomposite membranes were observed by scanning electron microscopy. Membranes were immersed in liquid nitrogen, and then fractured and gold sputter-coated before the SEM analysis.

Fourier-transform infrared (FT-IR)

A Perkin-Elmer Spectrum 100 FT-IR instrument was used to characterize the functional structure and the chemical groups in the PVA and PVA-SiO$_2$ nanocomposite membranes. The wave range of the FTIR spectra was between 4000 and 650 cm^{-1}.

Thermogravimetric analysis

The thermal properties of the PVA and PVA-SiO$_2$ nanocomposite membranes were investigated using Exstar TG/DTA 6300. TGA studies were conducted under a continuous nitrogen flow with a 10 °C min^{-1} heating rate from 25 to 600 °C.

Pervaporation experiments

Pervaporation experiments for PVA and PVA-SiO$_2$ nanocomposite membranes were carried out at 30, 40 and 50 °C. The schematic representation of the pervaporation setup is given elsewhere [23]. The feed tank was kept at a constant temperature in a water bath, and the feed mixture was fed to the stainless-steel membrane cell with a peristaltic pump. The effective membrane area of the membrane cell was 23 cm^2. The synthetic seawater mixture was prepared in our laboratory, and the salt concentration was 35 g L^{-1} [7,24]. The pressures on the feed and permeate sides of the membrane were kept at atmospheric pressure and ≤1 Torr, respectively, and the pressure on the permeate side was measured by a Vacuubrand DVR-2 digital vacuum meter. Samples were collected every hour in Dewar traps containing liquid nitrogen and were weighed accurately. Permeation fluxes (J) were calculated using the following equation:

$$J = \frac{W}{At} \qquad (1)$$

where W, A and t are the permeate amount (g), membrane's effective area (m^2) and the time interval (h), respectively. The salt rejection (R) was calculated by the conductivity method using the following equation:

$$R(\%) = 100\frac{C_f - C_p}{C_f} \qquad (2)$$

where C_f and C_p are salt concentrations in the feed and permeate, respectively. The pervaporation select-

ivity (α_i) was calculated using the following equation [25,26]:

$$\alpha_i = \frac{x_i / (1 - x_i)}{y_i / (1 - y_i)} \qquad (3)$$

where x and y are the weight fraction of component i in feed and permeate, respectively. The permeance of membrane (P_i/l) was determined according to Eq. (4) [25,27], assuming ideal solution (γ_{water} =1) for NaCl solution of 35 g/L [28]:

$$\frac{P_i}{l} = \frac{J_i}{x_i \gamma_i P_i^{sat} - y_i P^p} \qquad (4)$$

where P_i, l, γ_i and P^p are the membrane permeability, membrane thickness, activity coefficient and permeate pressure, respectively. The term $y_i P^p$ was ignored, as the permeate pressure was maintained at ≤1 Torr. The saturated vapor pressure (P_i^{sat}) can be calculated with the Antoine equation [29]:

$$\log(P_i^{sat} / \text{bar}) = A - \frac{B}{T + C - 273.15} \qquad (5)$$

where T is the temperature in Kelvin. A, B and C are the Antoine constants, and are given in Table 1 [29].

Table 1. Antoine constants for water [29]

Antoine coefficient		
A	B	C
5.11564	1687.537	230.17

RESULTS AND DISCUSSION

SEM Results

The cross-sectional SEM images of pristine PVA membranes (a) and PVA-SiO$_2$ nanocomposite membranes (b) are presented in Figure 2.
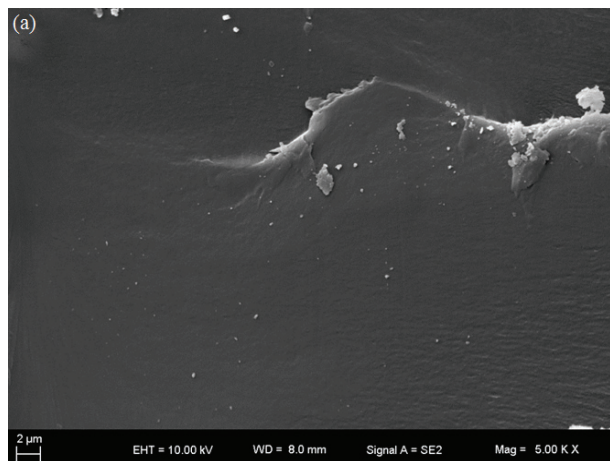
Figure 2a shows that the structure of the pristine PVA membrane is defect-free and smooth. Figure 2b shows homogeneous distribution of the nanomaterials within the polymer matrix. No particle agglomeration was observed.

FT-IR Results

The FT-IR spectra of the PVA and PVA-SiO$_2$ nanocomposite membranes are shown in Figure 3. The spectra can be divided into 4 main regions: I. hydroxyl groups (-OH), II. methylene groups (-CH$_2$), III. aldehyde groups (-CHO) and IV. acetal/ether groups (-COC), corresponding to 3000-3600 cm^{-1}, 2900-3000 cm^{-1}, 1650-1750 cm^{-1} and 1000-1100 cm^{-1} wavenumbers, respectively.

The FT-IR analysis of both PVA and PVA-SiO$_2$ nanocomposite membranes showed a broad peak between 3200 and 3300 cm^{-1}, indicating stretching of the hydroxyl groups of the polymer. In all spectra, the reflection peaks at approximately 2910, 2940 and 1418 cm^{-1} were assigned to a stretching vibration and flexural vibration of methylene (-CH) (the main structure of PVA), respectively [30]. The sharp peak observed at approximately 1700 cm^{-1} is assigned to C=O expansion band caused by ester groups [31]. This stretch is smaller in PVA with a higher degree of hydrolysis due to the lower number of acetate groups. The appearance of the ether/acetal peak indicates that crosslinking occurs between aldehyde groups and hydroxyl groups in the polymer [32-34]. The intensity of the peak at 1141 cm^{-1} is controlled by the crystalline segment of the polymer chains. This peak is related to the C-C and C-O bonds in the main carbon chain [22] and is constant for both PVA and PVA--SiO$_2$ nanocomposite membranes because the crystal structure of the polymer is the same for all samples. The peaks observed at approximately 3300 and 1100
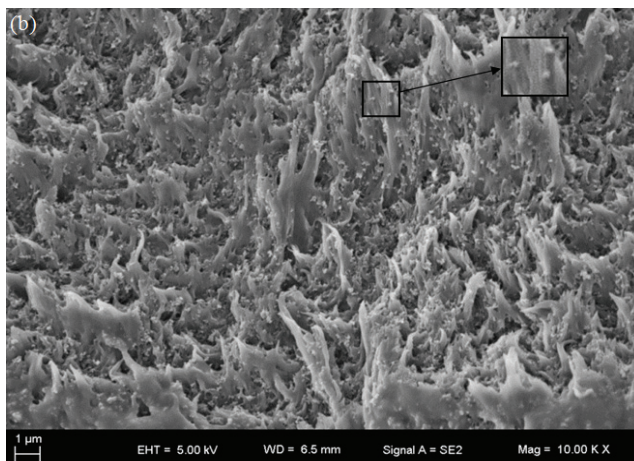

Figure 2. SEM images of PVA (a) and PVA-SiO$_2$ nanocomposite membranes (b).
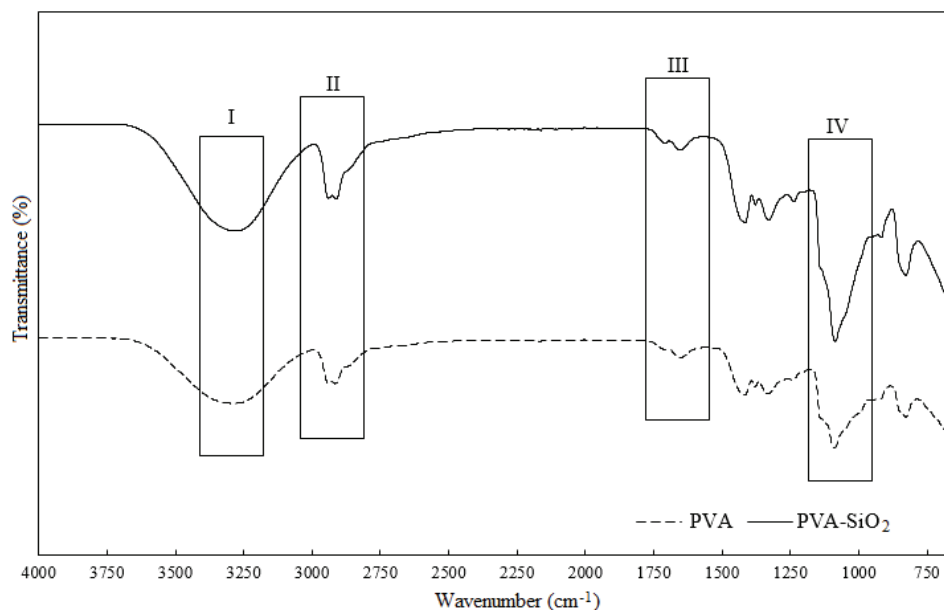
Figure 3. FT-IR spectra of PVA and PVA-SiO$_2$ nanocomposite membranes.

cm^{-1} are attributed to hydroxyl (-OH) groups and Si-O-Si stretching modes for PVA-SiO$_2$. A reduction in the intensity of the -OH and Si-O-Si groups was observed [34]. The peaks between 1000-450 cm^{-1} are attributed to the stretching vibrations of Si-O-Si. The peak at approximately 3440 cm^{-1} shifted to a lower wave number with the increase in nano-SiO$_2$ content, indicating an increase in intermolecular hydrogen bonds between nano-SiO$_2$ and PVA [35].

TGA Results

Figure 4 shows the TGA thermographs of the PVA and PVA-SiO$_2$ nanocomposite membranes. The thermal degradation profiles of both membranes revealed three weight loss stages.

The first weight loss step observed between 80-160 °C is due to the evaporation of bound and free water in the polymeric matrix and resulted in a loss of approximately 8.2 wt.% for PVA and for 26.3 wt.% PVA-SiO$_2$ (weight losses not shown). Primary decomposition of the PVA chain started at approximately 250 °C and is assigned to the elimination of side-groups of the polymer chain [36]. Total weight loss of the PVA membrane was approximately 74 wt.% and occurred at 400 °C. This first degradation step of PVA was followed by a final decomposition corresponding to the breakdown of the main polymer chain [37]. The decomposition of the main PVA chain started at 400 °C for PVA and 500 °C for PVA-SiO$_2$, and the weight
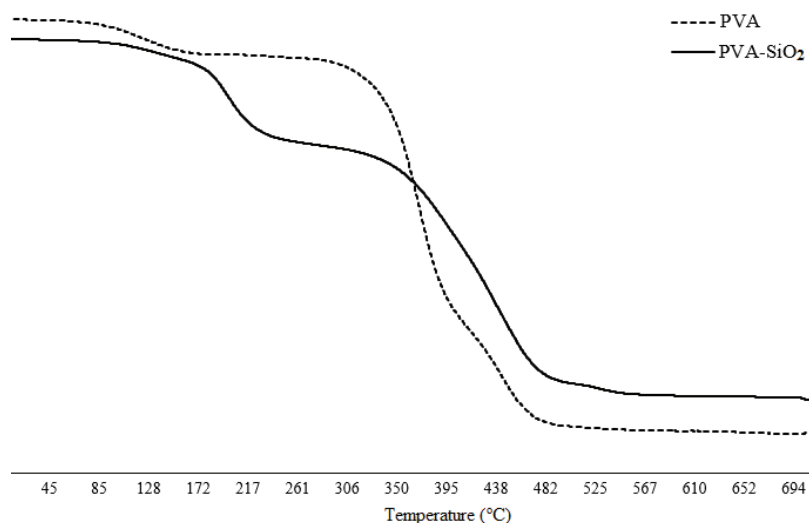

Figure 4. TGA thermographs of the PVA and PVA-SiO$_2$ nanocomposite membranes.

193

loss profiles of the PVA and PVA/SiO$_2$ nanocomposite membranes were similar. The shift towards the higher degradation temperature for the PVA-SiO$_2$ nanocomposite membrane is assigned to improved thermal stability due to the incorporation of SiO$_2$ nanomaterial into the PVA matrix.

Pervaporation results

The pervaporation desalination experiments were carried out at 30, 40, and 50 °C for PVA and PVA-SiO$_2$ nanocomposite membranes. Figure 5 shows the permeate water flux (a) and salt rejection (b) values of the PVA and PVA-SiO$_2$ membranes as a function of temperature for desalination of 35 g L^{-1} synthetic seawater.

Figure 5a shows that permeation rates increase with increasing temperature for both membranes as the mobility of the polymer chain and the solubility and diffusivity of water molecules through the polymeric matrix increase [38]. Salt rejection values obtained for PVA and PVA-SiO$_2$ membranes are shown in Figure 5b. Owing to the trade-off relationship between flux and selectivity for membrane processes, salt rejection values decrease with increasing temperature. This is related to the enhanced polymer

chain mobility that allows free ion transit. It is clear from Figure 5a and b that, with the nano-SiO$_2$ incorporation into the PVA matrix, both water flux and salt rejection increased due to the nanoporous and highly hydrophilic structure of the nanomaterial that rejects salt passage. A permeate flux of 4.93 kg m^{-2} h^{-1} was obtained for the PVA-SiO$_2$ membranes at 50 °C, and a salt rejection rate of >99% was observed for all temperatures.

Figure 6a and b illustrate the effects of temperature on permeance and selectivity, respectively. Based on the solution-diffusion model, the permeation flux depends on the solubility and diffusivity of components in the membrane. The permeances of both membranes decrease with the increasing of temperature, except for the permeance of PVA-SiO$_2$ membrane at temperature of 50 °C because the decrease in solubility is higher than the increase in diffusivity [39]. In contrast, the permeance of PVA-SiO$_2$ membrane increase at 50 °C as the permeation flux through PVA-SiO$_2$ membrane increases significantly from 40 to 50 °C. This also implies that the increase in the diffusivity is able to compensate the decreasing in the solubility [39,40]. As can be seen from Figure 6b, the selectivity of the PVA-SiO$_2$ membrane evidently dec-
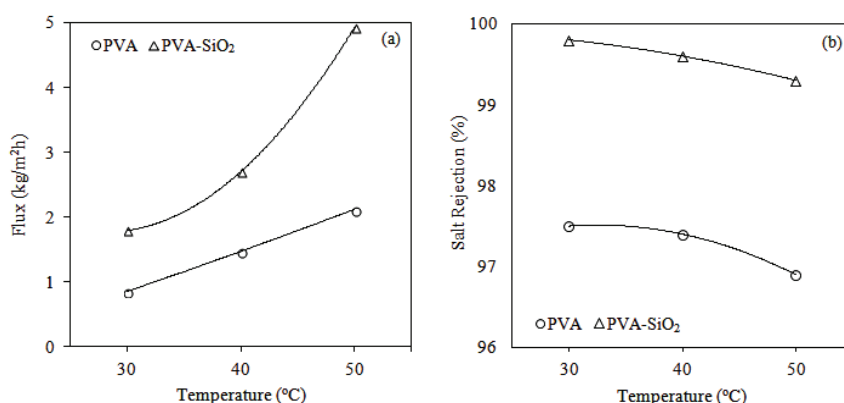

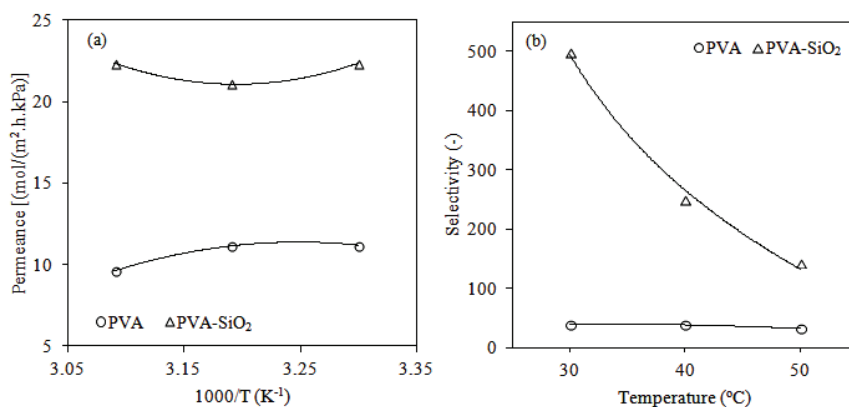Figure 5. Flux (a) and salt rejection (b) results of PVA and PVA-SiO$_2$ nanocomposite membranes.

Figure 6. Permeance (a) and selectivity (b) results of PVA and PVA-SiO$_2$ nanocomposite membranes.

reases with an increase in temperature, while selectivity decreases slightly for the PVA membrane, as the frequency and amplitude of the polymer chain mobility increase with increasing temperature.

Table 2 compares the desalination performance of the PVA-SiO$_2$ nanocomposite membrane with literature results based on pervaporation-based desalination. Considering the membrane thickness and temperature values, the PVA-SiO$_2$ membranes exhibited a good performance with high salt rejection and water flux.

CONCLUSION

The aim of this study was to prepare a membrane with high desalination performance. PVA was selected as the polymer matrix for its high hydrophilic nature, high thermal, mechanical, and chemical resistance, and great film-forming properties. Nanocomposite membranes were prepared with nano-sized SiO$_2$ and the effects of nanomaterial incorporation into a PVA matrix and temperature on water flux and salt rejection were investigated. Pervaporation experiments were carried out at different temperatures and the performance data for PVA-SiO$_2$ nanocomposite membranes were compared with pristine PVA membranes.

The pervaporation results exhibited that nano SiO$_2$ filler positively affected the membrane separation performance. The nano-SiO$_2$ incorporation into the PVA matrix increased the permeate flux values for all temperatures and salt rejection values >99% were obtained. The nanocomposite membrane seems to have much better salt rejection compared to pristine membranes. In addition, the TGA profiles showed that the decomposition temperature of the PVA membranes was improved with nano-SiO$_2$ incorporation. In conclusion, the pervaporation desalination results obtained using nano-SiO$_2$-filled PVA membranes are promising for seawater desalination.

REFERENCES

[1] E. Drioli, A.I. Stankiewicz, F. Macedonio, J. Membr. Sci. 380 (2011) 1-8

[2] Y. Li, L. Zhu, J. Taiwan Inst. Chem. Eng. 80 (2017) 867--874

[3] H. Cherif, J. Belhadj, In Sustainable Desalination Handbook-Plant Selection, Design and Implementation, Ch. 15, B.G. Gude, Ed., Butterworth-Heinemann: Oxford, 2018, pp 527-559

[4] J.O. Brotto, N. Padoin, C. R. Rambo, C. Soares, Water Supply 19 (2018) 1221-1228

[5] T. Humplik, J. Lee, S.C. O'Hern, B.A. Fellman, M.A. Baig, S.F. Hassan, M.A. Atieh, F. Rahman, T. Laoui, R. Karnik, E.N. Wang, Nanotechnology 22 (2011) 292001

[6] A.D. Khawaji, I.K. Kutubkhanah, J.M. Wie, Desalination 221 (2008) 47-69

[7] Q. Wang, N. Li, B. Bolto, M. Hoang, Z. Xie, Desalination 387 (2016) 46-60

Table 2. Performance comparison of various membranes in the pervaporation desalination studies; PVA, poly(vinylalcohol); PAN, polyacrylonitrile; GO, graphene oxide; CNT, carbon nanotube; PVDF, poly(vinylidene flouride); GA, glutaraldehyde; PEBA, poly(ether--block-amide). Model solutes are NaCl, Na$_2$SO$_4$ and MgCl$_2$

Membrane	NaCl content	Temperature (°C)	Thickness (μm)	Water flux	Salt rejection (%)	Reference
NaA zeolite	Seawater	69	-	1.9 kg m^{-2} h^{-1}	99.9	[17]
PVA/maleic anhydride/silica	2 g L^{-1}	20-65	10	6.9-11.7 kg m^{-2} h^{-1}	99.5-99.9	[15]
PVA/PAN	5 g L^{-1}	Room temperature	0.62-12.9	8.53 L m^{-2} h^{-1}	99.9	[19]
	35 g L^{-1}			7.36 L m^{-2} h^{-1}	99.8	
	50 g L^{-1}			5.81 L m^{-2}h^{-1}	99.8	
PVA	30 g L^{-1}	70	0.1	7.4 kg m^{-2} h^{-1}	99.9	[18]
PVA/Silica	2 g L^{-1}	60	4.9	20.6 L m^{-2}h^{-1}	99.9	[41]
	30 g L^{-1}			10.4 L m^{-2} h^{-1}	99.9	
PVA/PAN	35 g L^{-1}	70	-	11.2 kg m^{-2} h^{-1}	99.8	[42]
	100 g L^{-1}					
Chitosan/GO	5 wt.%	81	10-13	30.0 kg m^{-2}h^{-1}	99.99	[43]
PVA/GA/Laponite	3 wt%	70	-	58.6 kg m^{-2} h^{-1}	99.9	[44]
PVA/CNT	35 g L^{-1}	22	19	6.96 kg m^{-2} h^{-1}	99.91	[24]
PVA/PVDF	100 g L^{-1}	80	0.3	13.7 L m^{-2} h^{-1}	>99	[45]
			0.8	12.1 L m^{-2} h^{-1}		
			2.0	8.1 L m^{-2} h^{-1}		
PEBA	0-200 g L^{-1*}	25-65	40-90	0.5-1.7 kg m^{-2} h^{-1}	99.9	[46]
PVA/SiO$_2$	35 g L^{-1}	50	100	4.93 kg m^{-2} h^{-1}	99.3	This study

[8]   R.Y.M. Huang, Pervaporation Membrane Separation Process, Elsevier, Amsterdam, 1991

[9]   R.D. Noble, S.A. Stern, Membrane Separations Technology, Principles and Applications, Elsevier, Amsterdam, 1995

[10] B. Yilman, F.U. Nigiz, A. Aytaç, N.D. Hilmioglu, Water Supply 19 (2018) 1229-1237

[11] F.U. Nigiz, N.D. Hilmioglu, Desalin. Water Treat. 57 (2016) 4749-4755

[12] M. Maghami, A. Abdelrasul, In Zeolites and Their Applications, Ch. 7, M.N. Rashed, Ed., IntechOpen Ltd: London, 2018, pp. 115-134

[13] L.Y. Ng, A.W. Mohamad, C.P. Leo, N. Hilal, Desalination 308 (2013) 15-33

[14] J.H. Jhaveri, Z.V.P. Murthy, Desalin. Water Treat. 57 (2016) 26803-26819

[15] Z. Xie, M. Hoang, T. Duong, D. Ng, B. Dao, S. Gray, J. Membr. Sci. 383 (2011) 96-103

[16] Z. Xie, D. Ng, M. Hoang, T. Duong, S. Gray, Desalination 273 (2011) 220-225

[17] C.H. Cho, K.Y. Oh, S.K. Kim, J.G. Yeo, P. Sharma, J. Membr. Sci. 371 (2011) 226-238

[18] S.G. Chaudhri, B.H. Rajai, P.S. Singh, Desalination 367 (2015) 272-284

[19] B. Liang, K. Pan, L. Li, E.P. Giannelis, B. Cao, Desalination 347 (2014) 199-206

[20] B. Tirnakci, Master's thesis, Yildiz Technical University, Istanbul, 2017

[21] C.-K. Yeom, K.-H. Lee, J. Membr. Sci. 109 (1996) 257-265

[22] E.F. Reis, F.S. Campos, A.P. Lage, R.C. Leite, L.G. Heneine, W.L. Vasconcelos, Z.I.P. Lobato, H.S. Mansur, Mater. Res. 9 (2006) 185-191

[23] Y. Salt, E. Arcevik, B. Ekinci, Can. J. Chem. Eng. 92 (2014) 503-510

[24] G. Yang, Z. Xie, M. Cran, D. Ng, S. Gray, J. Membr. Sci. 579 (2019) 40-51

[25] P. Das, S.K. Ray, S.B. Kuila, H.S. Samanta, N.R. Singha, Sep. Purif. Technol. 81 (2011) 159-173

[26] R.S. Veerapur, M.B. Patil, K.B. Gudasi, T.M. Aminabhavi, Sep. Purif. Technol. 58 (2008) 377-385

[27] G. Jyoti, A. Keshav, and J. Anandkumar, J. Eng. (2015), Article ID 927068

[28] O. Miyawaki, A. Saito, T. Matsuo, K. Nakamura, Biosci. Biotech. Biochem., 61 (1997) 466-469

[29] B.E. Poling, J.M. Prausnitz, J.P. O'Connell, The Properties of Gases and Liquids, McGraw-Hill, NewYork, 2001

[30] L. Zhu, J. Wang, L. Guo, J. Shen, Adv. Mater. Res. 239--242 (2011) 1956-1959

[31] A. Şahin, I. Ar, J. Therm. Sci. Tech. 34 (2014) 153-162

[32] C.K. Yeom, K.H. Lee, J. Appl. Polym. Sci. 67 (1998) 209--219

[33] B. Smith, Infrared Spectral Interpretation: A Systematic Approach, CRC Press, New York, 1999

[34] O. Farid, F. Mansour, M. Habib, J. Robinson, S. Tarleton, J. Environ. Chem. Eng. 4 (2016) 293-298

[35] S. Tang, P. Zou, H. Xiong, H. Tang, Carbohydr. Polym. 72 (2008) 521-526

[36] C.C. Yang, Y.J. Li, T.H. Liou, Desalination 276 (2011) 366-372

[37] C.C. Yang, J. Membr. Sci. 288 (2007) 51-60

[38] A. Huang, B. Feng, J. Membr. Sci. 548 (2018) 59-65

[39] J. Xu, C. Gao, X. Feng, J. Membr. Sci. 352 (2010) 197-204

[40] D. T. Bui, A. Nida, K. C. Ng, K. J. Chua, J. Membr. Sci. 498 (2016) 254-262

[41] S.G. Chaudhri, J.C. Chaudhari, P.S. Singh, J. Appl. Polym. Sci. 134 (2017) 45718

[42] R. Zhang, B. Liang, T. Qu, B. Cao, P. Li, Environ. Technol. 40 (2017) 312-320

[43] X. Qian, N. Li, Q. Wang, S. Ji, Desalination 438 (2018) 83-96

[44] A. Selim, A.J. Toth, E. Haaz, D. Fozer, A., Szanyi, N. Hegyesi, P. Mizsey, Sep. Purif. Technol. 221 (2019) 201--210

[45] L. Li, J. Hou, Y. Ye, J. Mansouri, V. Chen, Desalination 422 (2017) 49-58

[46] D. Wu, A. Gao, H. Zhao, X. Feng, Chem. Eng. Res. Des. 136 (2018) 154-164.

BERK TIRNAKCI
YAVUZ SALT

Department of Chemical Engineering, Faculty of Chemical and Metallurgical, Yildiz Technical University, Davutpasa Campus, Esenler-Istanbul, Turkey

NAUČNI RAD

DOBIJANJE I KARAKTERIZACIJA PVA-SIO$_2$ NANOKOMPOZITNIH MEMBRANA ZA DESALINACIJU MORSKE VODE PERVAPORACIJOM

Pervaporacija je membranski proces koji nudi visok stepen razdvajanja i ima važan potencijal za tretman slanih izvora vode. U ovom radu, pripremljeni su poli(vinilalkohol) (PVA) i PVA-SiO$_2$ nanokompozitne membrane metodom livenja rastvora, koje su zatim korišćene u istraživanju desalinizacije sintetičke morsku vodu (35 g L^{-1}) na 30, 40 i 50 °C. Istraživani su efekti temperature i ugradnje SiO$_2$ na performanse pervaporacije polimernim nanokompozitnim membranama. Membrane su okarakterisane skenirajućom elektronskom mikroskopijom, infracrvenom spektroskopijom sa Furijeovom transformacijom i termogravimetrijskom analizom. U eksperimentima izvedenim na 50 °C, dobijen je fluks permeata od 4,93 kg m^{-2} h^{-1} sa uklanjanjem soli 99,3%. Najveće uklanjanje soli od 99,8% postignuto je na temperaturi od 30 °C. Rezultati su pokazali da su pervaporacione performanse PVA membrana izuzetno poboljšane ugradnjom nano-SiO$_2$ u polimernu matricu.

Ključne reči: desalinizacija, nano-SiO$_2$, nanokompozit, pervaporacija, poli(vinilalkohol), morska voda.

197